Light scattering in Intralipid-10% in the wavelength range of 400–1100 nm

Hugo J. van Staveren, Christian J. M. Moes, Jan van Marle, Scott A. Prahl, and Martin J. C. van Gemert

The absorption, scattering, and anisotropy coefficients of the fat emulsion Intralipid-10% have been measured at 457.9, 514.5, 632.8, and 1064 nm. The size and shape distributions of the scattering particles in Intralipid-10% were determined by transmission electron microscopy. Mie theory calculations performed by using the particle size distribution yielded values for the scattering and anisotropy coefficients from 400 to 1100 nm. The agreement with experimental values is better than 6%.

I. Introduction

Intralipid-10% is a fat emulsion that is used clinically as an intravenously administered nutrient. Sometimes, as in the research described in this paper, it is used for providing the scattering component in a tissue phantom to investigate propagation of light in tissue. The optical parameters of Intralipid-10%, namely, the absorption coefficient μ_a, the scattering coefficient μ_s, and the anisotropy coefficient g (the mean cosine of the scattering angle), have previously been investigated near the 630-nm wavelength.[1,2] This wavelength is used in photodynamic therapy, with haematoporphyrin derivative as a photosensitizer, as a treatment for cancer. The use of green light instead of red light for photodynamic therapy has been proposed, because green light is more effective for exciting haematoporphyrin.[3] Therefore further investigations into methods used in tissue optics will need well-characterized phantom materials for the entire optical wavelength range. The purpose of the present study is to obtain experimental values for μ_a, μ_s, and g for Intralipid-10% (Kabivitrum, Stockholm) at various wavelengths and to compare these values with those predicted by Mie theory and with data of other investigations.[1,2,4]

When the research was performed all authors were with the Academic Medical Center, Amsterdam, The Netherlands. C. J. M. Moes is now with the Polytechnics Institute 's Hertogenbosch, 's Hertogenbosch, The Netherlands. S. A. Prahl is now with the Wellman Laser Laboratories, Massachusetts General Hospital, Boston, Massachusetts 02114, and H.J. van Staveren is now with the Daniel den Hoed Cancer Center, Rotterdam, The Netherlands.

Received 12 February 1990.
0003-6935/91/314507-08$05.00/0.

Values for μ_s were obtained by measuring the collimated transmittance with a small numerical aperture detector as a function of diluted Intralipid-10% suspensions. Values of an effective attenuation coefficient (μ_{eff}) were obtained by measuring the fluence rate of an isotropic light source immersed in an infinite suspension of Intralipid-10% by using an added-absorber method.[1] Values for μ_a and g were then calculated based on (approximate) solutions to the transport equation in the P1 approximation (diffusion approximation) or the more accurate P3 approximation. The experiments used an Ar^+ laser for the 457.9- and 514.5-nm wavelengths, a He–Ne laser for the 632.8-nm wavelength, and a Nd:YAG laser for the 1064-nm wavelength. Mie theory calculations require precise knowledge of the particle size distribution of Intralipid-10%, which was determined by electron microscopy. The shape of the particles was approximately spherical, indicating that Mie theory is appropriate for calculating μ_s and g. These calculations were performed for 400–1100-nm wavelengths.

II. Methods and Materials

A. Experimental Procedures

1. *Collimated Transmission Measurements*

To determine the scattering coefficient of Intralipid-10%, we measured the collimated, transmitted, unscattered light in aqueous suspensions that were prepared by volumetrically diluting Intralipid-10% with distilled water (Fig. 1). Light from the Ar^+ laser (Spectra-Physics Model 2030) and the Nd:YAG laser (SLT-CL60) was delivered by optical fibers (600 μm). The He–Ne aiming beam of the Nd:YAG laser was

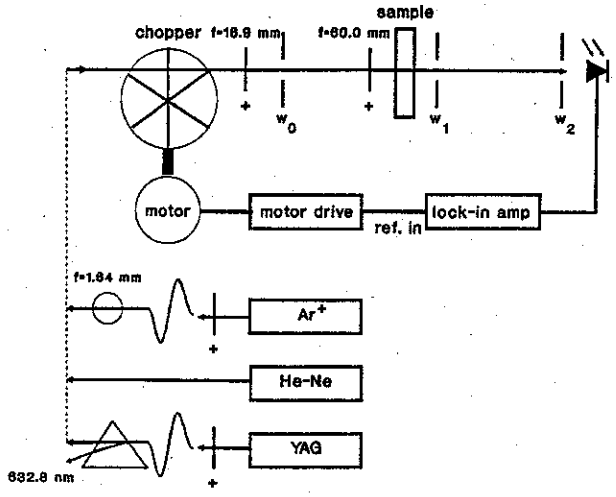

Fig. 1. Experimental setup for collimated transmission measurements to determine the scattering coefficient [$\mu_s(\lambda)$] of a scattering, nonabsorbing medium.

separated from the 1064-nm beam with a prism. The Ar^+ laser beam was collimated with a ball lens ($f = 1.64$ mm). The Ar^+ (or a separate He–Ne or Nd:YAG) laser beam was then chopped (2 kHz) and expanded ($\approx$15 mm for the Ar^+ and Nd:YAG laser beams, $\approx$9 mm for the He–Ne laser beam) before passing perpendicularly through a sample holder [with glass windows and sample thickness $d = 3.35(5)$ mm, with the He–Ne laser $d = 3.50(5)$ mm] filled with one of the Intralipid-10% suspensions. (Numbers in parentheses are the standard deviation uncertainties in the last digit of each quoted value.) Inside the beam expander a pinhole (100 μm), placed at the foci of the lenses, ensured that deviating beams introduced by the optical fibers were blocked. This arrangement reduced the beam divergence of the Ar^+ and Nd:YAG lasers to <5 mrad and the He–Ne laser near the diffraction-limited divergence of <75 μrad. The collimated transmittance was detected by a photodiode (BPW 34, sensitive for wavelengths from 400 to 1100 nm) placed 2.87(1) m from the sample. Two pinholes, one placed immediately behind the sample holder [1.50(5) mm] and one placed in front of the photodiode [0.50(5) mm], provided a small angular aperture [$3.8(3) \times 10^{-7}$ sr]. In this way only the fraction of the incident beam that was neither scattered nor absorbed was detected by the photodiode. The signal of the photodiode was fed into a lock-in amplifier (EG&G/PARC Model 5209), which tracked the frequency of the chopper (EG&G/PARC Model 196). The collimated irradiance (E_c, in watts per square meter) detected by the photodiode is given by

$$E_c = E_w \exp[-(\mu_a + \mu_s)cd], \quad (1)$$

with E_w the irradiance when the sample holder is filled with distilled water, c the concentration of the Intralipid-10% suspension, and d the geometrical path length in the sample holder. [Concentration is defined as the ratio between volume (in milliliters) of the stock solution (Intralipid-10%) and total volume (in liters) of stock solution plus solvent (water). It is also quoted as the volume percentage of the stock solution.] If absorption is negligible relative to scattering ($\mu_s \gg \mu_a$), then the slope of a plot of $\ln(E_c/E_w)$ versus (cd) determines μ_s. This condition is demonstrated by using the added-absorber technique described in Subsection II.A.2. Because all measurements have been normalized to E_w, additional absorption (or scattering) by water has virtually no influence on the value of the experimental scattering coefficient.

2. *Fluence Rate Measurements*

The light distribution in an absorbing and scattering medium is described by the radiative transfer equation.[5] For a point source in an infinite medium an analytic solution of this integrodifferential equation can be obtained. In the P1 approximation (=the diffusion approximation),[5] scattering of light is approximated by the sum of an isotropic part and a small anisotropic part, and the radiation inside the medium is assumed to be (nearly) diffuse. This approximation is expected to yield reasonably accurate results for the fluence rate distribution in regions far from sources and boundaries provided that the reduced albedo a' is close to 1 [$a' = \mu_s'/(\mu_s' + \mu_a)$, where $\mu_s' = \mu_s(1 - g)$] which implies that $\mu_s' \gg \mu_a$. If these conditions are ill satisfied, the P3 approximation[6] will be expected to yield more accurate results. As a' decreases with increasing wavelength for Intralipid-10% suspensions, the P1 approximation should eventually break down. The results for μ_a and g of both approximations are compared with each other: thus the wavelength limit can be assessed where the P1 approximation starts to be of limited accuracy.

To determine the absorption and the anisotropy coefficients of Intralipid-10%, we measured the light-energy fluence rate of an isotropic light source immersed in an aqueous suspension of Intralipid-10% with and without Evans Blue (a purely absorbing medium) as a function of the distance from the light source (Fig. 2). The Ar^+ (or He–Ne or Nd:YAG) laser beam was chopped (2 kHz) and coupled into a fiber (600 μm). A sphere of highly scattering material (sphere diameter 3 mm) was attached to the distal end of this fiber, thereby producing an isotropic output.[2,7] This fiber tip was positioned accurately in a vertical direction. To measure the fluence rate, we used another fiber (200 μm) with a sphere of scattering material (sphere diameter, 1 mm) attached to the fiber end. This fiber tip was positioned in the x, y, and z directions with an accuracy of better than 0.1 mm. Isotropicity of both scattering spheres was checked by measuring the angular-light distribution (deviations from the mean intensity of ±20% for the light source and ±15% for the detector). Light received by the detecting fiber was detected by a photodiode (BPW 34), and the signal was fed into the lock-in amplifier

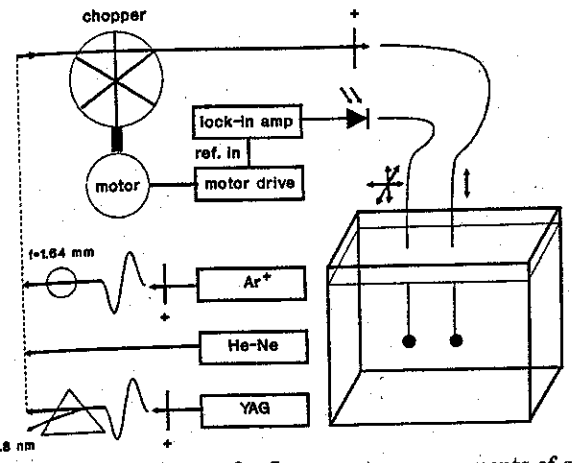

Fig. 2. Experimental setup for fluence rate measurements of an isotropic light source in an infinite medium to determine the absorption $[\mu_a(\lambda)]$ and the anisotropy $[g(\lambda)]$ coefficients of the medium by using an added absorber.

which tracked the frequency of the chopper. Both fibers were placed in a Perspex tank (20 cm × 20 cm × 16 cm) filled with 5.5 L of an Intralipid-10% suspension. Wall effects were determined to be negligible by changing the reflectivity of the walls. Measurements were performed in an aqueous suspension of 3% Intralipid-10% and in an aqueous suspension of 3% Intralipid-10% containing 5.15 mg/L Evans Blue. Fluorescence from Intralipid-10% or Evans Blue is believed to be negligible but was not clearly ruled out. The two suspensions have different scattering and absorption coefficients at the four investigated wavelengths. For the 1064-nm wavelength a suitable absorbing medium was not found to be available, so fluence rates are measured only in the pure 3% suspension of Intralipid-10% at this wavelength. (Ink is often used as an absorber for the Nd:YAG laser wavelength. However, it was noted that ink has significant scattering at 1064 nm. Other absorptive dyes at this wavelength could not be dissolved in water.) As a consequence, μ_a and g could not be determined directly for this wavelength.

The fluence rate (Ψ, in watts per square meter) at a distance (r) from the point source in these infinite turbid media is given by[5]

$$\Psi(r) = \frac{B}{r}\exp(-\mu_{\text{eff}} r), \tag{2}$$

where

$$B = \frac{3P_0[\mu_a + \mu_s(1-g)]}{16\pi^2},$$

with μ_{eff} the effective attenuation coefficient defined below [Eqs. (3) and (4)], P_0 the power of the point source, and μ_a as the total absorption coefficient of Intralipid-10% ($\mu_{a\text{IL}}$) and added Evans Blue ($\mu_{a\text{EB}}$). The slope of a plot of $\ln(r\Psi/B)$ versus r gives the effective attenuation coefficient μ_{eff}. Measuring the fluence rate in the Intralipid-10% suspensions with and without the added absorber gives μ_{eff} and μ_{eff0}, respectively. In the P1 approximation, the following set of equations must then be solved for $\mu_{a\text{IL}}$ and g (Ref. 5):

$$\mu_{\text{eff0}}^2 = 3\mu_{a\text{IL}}[\mu_{a\text{IL}} + (\mu_{\text{ext}} - \mu_{a\text{IL}})(1-g)],$$
$$\mu_{\text{eff}}^2 = 3(\mu_{a\text{IL}} + \mu_{a\text{EB}})[\mu_{a\text{IL}} + \mu_{a\text{EB}} + (\mu_{\text{ext}} - \mu_{a\text{IL}})(1-g)]. \tag{3}$$

Values for the extinction coefficients $\mu_{\text{ext}} = \mu_s + \mu_{a\text{IL}}$ are obtained from the collimated transmission measurements. Values for $\mu_{a\text{EB}}$ are determined similarly at 514.5- and 632.8-nm wavelengths and at the 457.9-nm wavelength with a spectrometer. In the P3 approximation, μ_{eff} [Eq. (2)] is given by[6]

$$\mu_{\text{eff}}^2 = [9\gamma_0\gamma_1 + 4\gamma_0\gamma_3 + \gamma_2\gamma_3 - [(9\gamma_0\gamma_1 + 4\gamma_0\gamma_3 + \gamma_2\gamma_3)^2 - 36\gamma_0\gamma_1\gamma_2\gamma_3]^{1/2}]/18, \tag{4}$$

where γ_0 to γ_3 follow from

$$\gamma_n = (2n+1)[\mu_a + \mu_s(1-g^n)], \qquad n = 0, 1, 2, 3,$$

with $\mu_a = \mu_{a\text{IL}} + \mu_{a\text{EB}}$. The values of $\mu_{a\text{IL}}$ and g were then found by solving Eqs. (3) and (4) numerically.

B. Determination of the Particle Size and Shape Distribution

Electron microscopy permits determination of both the size and the shape of the scattering particles in Intralipid-10%. Freeze fracture was used to make Intralipid-10% accessible for electron microscopy.[8] Intralipid-10% samples were cryoprotected (prevented from forming ice crystals) with 2–3 M of sucrose, fractured at 170 K in a vacuum chamber at 10^{-6} Pa, replicated with platinum at 45°, and strengthened with carbon. The platinum replicas of the fracture planes were studied at a magnification of 18,000× at 100 kV in a Philips EM 420 electron-microscopy device. From each of the 10 Intralipid-10% preparations that were made, 10–15 transmission electron microscope photographs were taken and magnified at 6×. From these photographs 1436 particle sections were measured (10–14 particles per photograph) by tracing them with a digitizer [MOP videoplan (Kontron), spatial resolution 0.9 nm]. The (numerous) particle sections below ≈20-nm diameter were disregarded. A histogram of the number of particle sections within a diameter interval versus the median diameter of that interval (d_i) gives the particle (section) size distribution. Although the measured particle sections actually belong to particles with a greater diameter [if the probability of splitting is homogeneously distributed along a particle's radius, the expected section diameter (ϵ_d) is $\epsilon_d = \frac{1}{2}D\sqrt{3}$ with a standard deviation [$\sigma(d)$] of $\sigma(d) = D/6$, where D is the particle diameter], correction for the splitting of

the scattering particles was omitted (Section IV). All measured particle sections were classified into 14 particle diameters to ensure that most classes contained at least a few particle sections and to reduce calculations. A form factor [perimeter eccentricity (PE)] was computed for the particle sections by using the digitizer data. This form factor for an area A with perimeter s is defined as[9]

$$PE = \frac{4\pi A}{s^2}. \tag{5}$$

The closer the form factor is to 1 (for any nonspherical shape $PE < 1$), the closer the particles are to a spherical shape. A plot of the form factor versus the particle diameter (Fig. 8 below) delineates the extent to which Mie theory is applicable for calculating the scattering parameters of Intralipid-10%.

C. Mie Theory Simulations

The constituents of 500 mL of Intralipid-10%, according to the manufacturer, are 11.25 g of glycerin, 6 g of lecithin, 50 g of soybean oil, and 430.5 g of water [respectively, 8.92, 5.82, 53.94, and 431.33 mL (Refs. 10 and 11)]. The glycerin is dissolved into individual molecules in the water and does not scatter light. The difference in the refractive index of this water–glycerin solution from that of pure water has no measurable influence on the scattering parameters. The scattering particles consist of soybean oil encapsulated within a monolayer membrane of lecithin with a thickness of approximately 2.5–5 nm [Fig. 3(a)].[12] This explains the name intralipid (meaning inside the lipid). In Intralipid-10%, approximately half of the amount of lecithin is used for encapsulating the soybean oil, and the excess of lecithin forms small bilayer vesicles [Fig. 3(b)]. A concentric-spheres model has not been included in the Mie calculations because of the unknown refractive index of lecithin.[13] Therefore we assumed that lecithin has the same refractive index as soybean oil. If lecithin does not absorb light at the investigated wavelengths, the influence of this shell on scattering should be negligible. In the calculations of the scattering parameters μ_s and g, the volume occupied by lecithin in a particle is included. Despite the fact that only part of the lecithin is encapsulating the soybean oil, we had to make the assumption that all the lecithin is used for encapsulating the soybean oil.

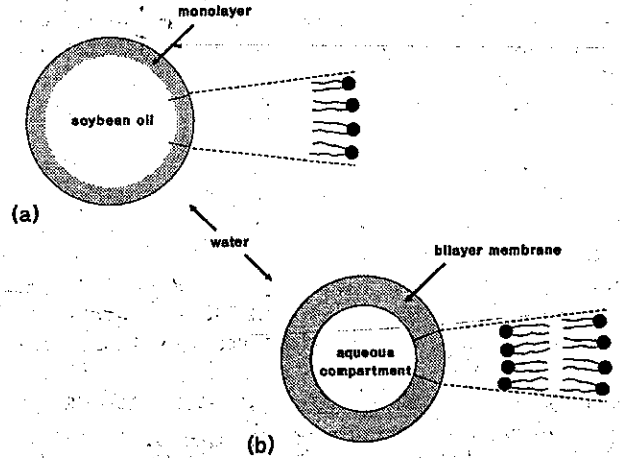

Fig. 3. (a) Model of an Intralipid-10% particle after sonification of a solution of soybean oil, lecithin, glycerin, and water. (b) Model of a lipid vesicle in water.[12]

Mie theory provides an exact solution for the scattering and the anisotropy coefficients of perfect spheres of arbitrary size.[14,15] To compare experimental results with Mie theory, we used a computer program to calculate Mie scattering parameters. [The rigorous Mie formulas are evaluated by a computer program of J. R. Zijp (State University Groningen, Groningen, The Netherlands).] This program requires the parameters

$$x = \frac{2\pi r n_{ext}}{\lambda_{vac}}, \qquad m = \frac{n_{sph}}{n_{ext}}, \tag{6}$$

where r is the radius of the sphere, λ_{vac} is the wavelength in vacuum, n_{sph} is the real part of the refractive index of the sphere, and n_{ext} is the refractive index of the (nonabsorbing) external medium (the suspending medium). Values for the radii of the spheres were found from electron microscopy. The refractive indices for the various wavelengths were calculated with the following dispersion formula (Cauchy[10]):

$$n(\lambda) = I + J/\lambda^2 + K/\lambda^4, \tag{7}$$

where $I_{soybean} = 1.451$, $I_{water} = 1.311$, $J = 1.154 \times 10^4$, $K = -1.132 \times 10^9$, and the wavelength (λ) is in nanometers. All constants in Eq. (7) are determined for both media by solving the equation using known refractive indices at three wavelengths. From values for x and m the computer program generated efficiency factors for scattering $Q_{sca}(r, \lambda)$, defined as the ratio between the scattering cross section with the geometrical cross section and the anisotropy factor $g(r, \lambda)$. The cross section for scattering $\sigma_{sca}(r, \lambda)$ of a particle is given by

$$\sigma_{sca}(r, \lambda) = \pi r^2 Q_{sca}(r, \lambda), \tag{8}$$

where πr^2 is the geometrical cross section. The total cross section for scattering per unit volume [$\mu_s(\lambda)$] and the anisotropy coefficient [$g(\lambda)$] for a suspension of particles with different (discrete) radii are then calculated by

$$\mu_s(\lambda) = N_0 \sum_{i=1}^{n} \sigma_{sca}(r_i, \lambda) f(r_i), \tag{9}$$

$$g(\lambda) = \frac{\sum_{i=1}^{n} g(r_i, \lambda)\, \sigma_{sca}(r_i, \lambda) f(r_i)}{\sum_{i=1}^{n} \sigma_{sca}(r_i, \lambda) f(r_i)}, \tag{10}$$

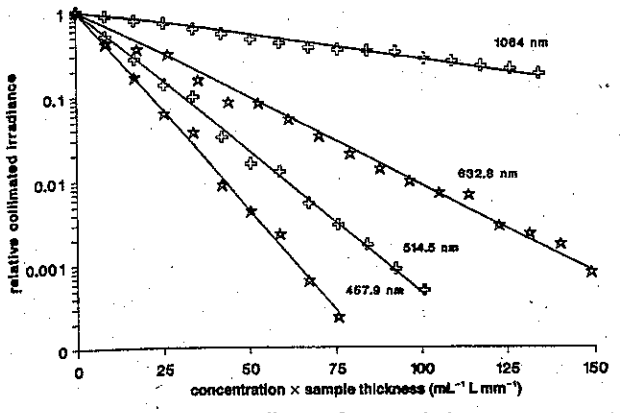

Fig. 4. Plot of data from collimated transmission measurements of diluted Intralipid-10% suspensions at the four investigated wavelengths. The slopes of the fitted lines give the extinction coefficients ($\mu_{ext} = \mu_s + \mu_a$).

where $f(r_i)$ is the fraction of particles with radius r_i and

$$\sum_{i=1}^{n} f(r_i) = 1$$

and with the particle density N_0 given by

$$N_0 = \frac{v}{\sum_{i=1}^{n} \frac{4}{3}\pi r_i^3 f(r_i)}, \tag{11}$$

where v is the volume of soybean oil plus the volume of lecithin per unit volume of suspension. The values of $f(r_i)$ are found from electron microscopy. The resulting values for $\mu_s(\lambda)$ and $g(\lambda)$ are valid only if the mean particle spacing is at least 3–5 particle diameters, which implies no shadowing of the particles.[14] The experimental conditions were chosen to obey this condition (concentration of Intralipid-10% less than $\approx 17-\approx 4\%$ for the wavelength range of 400–1100 nm; see Section III). Calculations for μ_s and g were performed between 400 and 1100 nm. Outside this wavelength region, the refractive index of soybean oil was unknown, and, in addition, the suspending medium for the particles (water) cannot be regarded any more as a nonabsorbing medium (μ_a of water below 4×10^{-2} mm^{-1} from 200 to 1000 nm),[16] which is a requirement for using Mie theory.

III. Results

Results from the collimated transmission experiments are shown in Fig. 4. Plotted on the logarithmic ordinate is the relative collimated irradiance (E_c/E_w) versus the product of volumetric dilution and sample thickness (cd). The data for each wavelength have been fitted to a line passing through the origin [the point (0, 1)]. The slopes of these lines yield $\mu_s(\lambda)$, as explained in Subsection II.A.1 (more precisely, the extinction coefficient $\mu_a + \mu_s$; see Table I).

Figure 5 shows the results of the fluence rate measurements of the Intralipid-10% suspensions with and without added absorber. Plotted, on the logarithmic ordinates, is the relative product of distance to the point source and fluence rate ($r\Psi/B$) versus distance to the point source (r). The slopes of the lines give the effective attenuation coefficients $\mu_{eff0}(\lambda)$ [2.66(2) × 10^{-2}, 1.97(2) × 10^{-2}, 2.11(2) × 10^{-2}, and

Table I. Survey of Experimental and Mie Theory Values of the Scattering [$\mu_s(\lambda)$], Anisotropy [$g(\lambda)$], and Absorption [$\mu_a(\lambda)$] Coefficients for Intralipid-10% Compared with Experimental Values of Other Investigations

This Work λ (nm)	μ_s (mL^{-1} L mm^{-1}) Experimental $\mu_{ext} \doteq \mu_s + \mu_a$	Experimental μ_s	Mie Theory	g Value Experimental P1 Approximation	Experimental P3 Approximation	Mie Theory	$\mu_s \times 10^5$ (mL^{-1} L mm^{-1}) Experimental P1 Approximation	Experimental P3 Approximation	Comments
457.9	0.109 (2)	0.109 (2)	0.104	0.872 (6)	0.871 (6)	0.829	1.88 (9)	1.87 (9)	P3 values have the calculated relative standard deviations of P1 values. For the 1064-nm wavelength, Mie values at 1060 nm. μ_a at 1064-nm wavelength, calculated with Mie value of g.
514.5	0.077 (1)	0.077 (1)	0.0813	0.812 (7)	0.807 (7)	0.799	0.99 (4)	0.96 (4)	
632.8	0.0476 (9)	0.0476 (9)	0.0498	0.796 (6)	0.768 (6)	0.731	1.69 (5)	1.49 (4)	
1064	0.0136 (3)	0.0131 (3)	0.0134			0.480	47 (9)	48 (9)	
Moes et al.[1] 632.8	0.0386 (4)	0.0386 (4)		0.71 (3)			6 (1)		
Star et al.[2] 630	0.055	0.055		0.83			0.95		
Flock et al.[4] 515	0.054 (8)	0.054 (8)		0.85			0.14		
632.8	0.034 (3)	0.034 (3)		0.825			0.018		

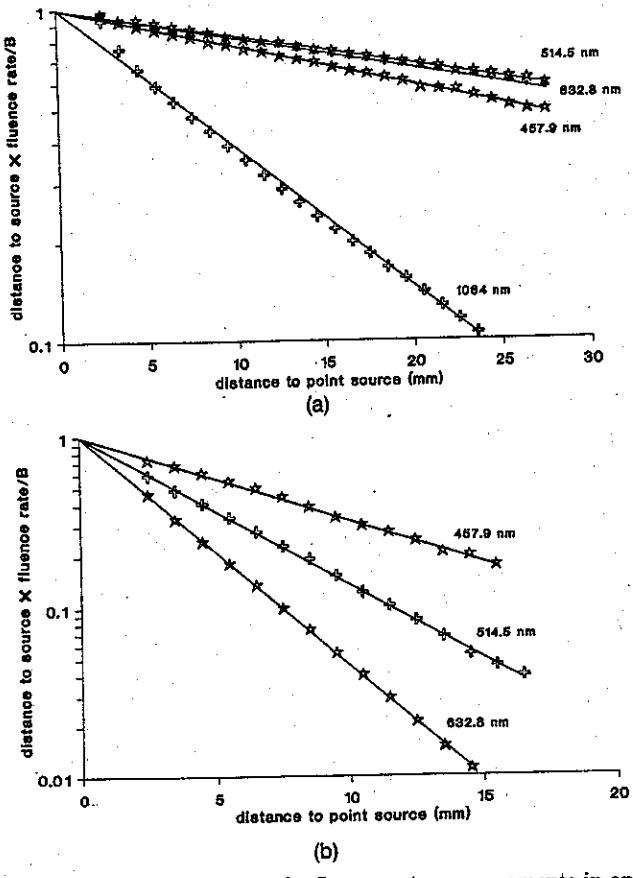

Fig. 5. Plot of data from the fluence rate measurements in an infinite suspension of 3% Intralipid-10% with and without added absorber at the four investigated wavelengths. The slopes of the fitted lines give the effective attenuation coefficients: (a) without added absorber, (b) with added absorber (Evans Blue).

$9.6(1) \times 10^{-2}$ mm^{-1} at, respectively, 457.9-, 514.5-, 632.8-, and 1064-nm wavelengths; Fig. 5(a)] and $\mu_{eff}(\lambda)$ [$1.13(2) \times 10^{-1}$, $1.99(2) \times 10^{-1}$, and $3.09(2) \times 10^{-1}$ mm^{-1} at, respectively, 457.9-, 514.5-, and 632.8-nm wavelengths; Fig. 5(b)]. As we mentioned in Subsection II.A.2, for the 1064-nm wavelength the effective attenuation coefficient was determined only for the Intralipid-10% suspension without added absorber. With known $\mu_s(\lambda)$ from the collimated transmission experiments and $\mu_{aEB}(\lambda)$ [$9.3(3) \times 10^{-3}$, $2.82(6) \times 10^{-2}$, and $8.4(1) \times 10^{-2}$ mm^{-1} for the Evans Blue solution at, respectively, 457.9-, 514.5-, and 632.8-nm wavelengths], $\mu_{aIL}(\lambda)$ and $g(\lambda)$ can be calculated [Eqs. (3) and (4)].

The experimental results and a comparison with the calculated results from Subsection II.C are summarized in Table I. In addition, a comparison was made with other investigations of Intralipid-10%.[1,2,4] The absorption coefficient μ_a at 1064 nm could be calculated by using the Mie value of g, so the reliability of this result depends on the accuracy of the calculations. As all μ_a are low compared with μ_s, the collimated transmission experiments yielded the scattering coefficients directly. Absorption measurements at 632.8 nm of purely obtained soybean oil, lecithin, glycerin, and water (according to the constituents' mixture of the Intralipid-10% manufacturer) resulte for Intralipid-10% in $\mu_a = 1.75 \times 10^{-5}$ mL^{-1} L mm^{-1} This value deviates 17% from the value calculated b the P3 approximation but <4% from that of the P approximation.

Figure 6 shows a typical electron-microscope photo graph of an Intralipid-10% preparation. This show the size differences in Intralipid-10% particles an their generally spherical shape. A shell structure not apparent (otherwise the fracture planes woul have been less smooth), which proves that a shar boundary (in the case of a bilayer membrane) b tween lecithin and soybean oil is absent. Hence follows that the layer of lecithin is a monolayer.

The histogram in Fig. 7 illustrates the partic (section) size distribution of Intralipid-10%. The nur ber of particle sections within a diameter interval 50 nm is plotted versus the median diameter of th interval (d_i). That there were no 625-nm diamet particles is not considered significant, because t last interval contains only one particle. The mea particle diameter of this distribution is 97(3) nm.

Figure 8 gives information on the particle shape Plotted on the ordinate is the form factor (PE) vers the mean diameter of that particle (d). The smalle particles show the largest deviation from a spheri shape. This is most likely due in part to inaccuracy tracing these particles and to digitizing errors (spat resolution 0.9 nm). The smallest particles are Ra leigh scatterers for the wavelengths of interest (ver cal lines, $d < 40$ nm for 400-nm and $d < 120$ nm 1100-nm wavelengths). Consequently the shape

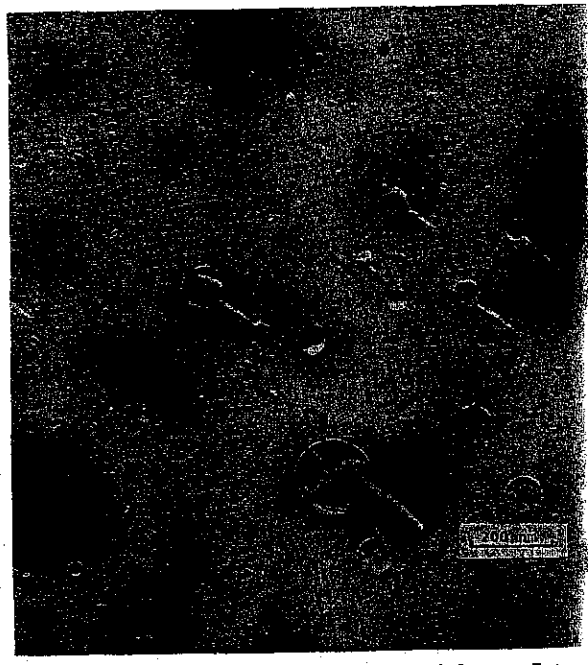

Fig. 6. Typical electron-microscope photograph from an Intra 10% preparation, containing the replica of fracture planes of droplets from Intralipid-10%. The shaded areas are remainde Intralipid-10% and chlorine, with which the platinum sheet cleaned. The black spots are due to etching of the platinum b chlorine.

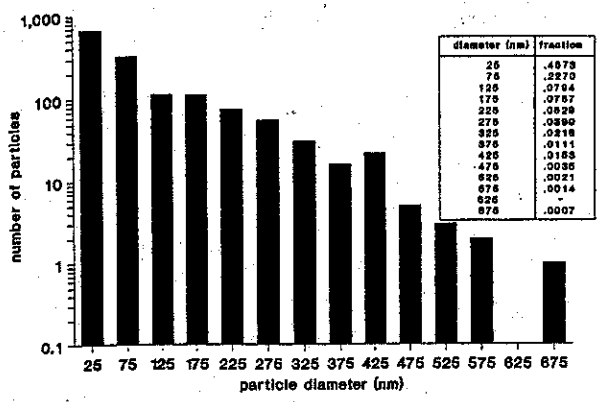

Fig. 7. Particle (section) size distribution of 1436 measured intralipid particles (sections) determined by transmission electron microscopy. For this sample, the mean with its standard deviation is 97(3) nm. This distribution is used with Mie theory to calculate the scattering parameters $\mu_s(\lambda)$ and $g(\lambda)$ for Intralipid-10%.

these particles is not important and does not affect the results of the scattering calculations. A form factor of 0.97 (horizontal line) implies, in case of ellipses, an axis ratio of 0.8. Up to this deviation from the spherical shape, the accuracy of Mie scattering calculations is not significantly influenced.[14] Therefore this particle shape distribution shows that Mie theory is applicable for calculating the scattering parameters of Intralipid-10%.

Figures 9 and 10 compare the Mie theory values of $\mu_s(\lambda)$ and $g(\lambda)$ for Intralipid-10% with the experimental values obtained above. In both figures the maximum deviation of the experimental values (P3 approximations) from the calculated values is $<6\%$ (457.9-nm data points). The plots of $\ln \mu_s(\lambda)$ versus $\ln \lambda$ (Fig. 9) and of $g(\lambda)$ versus λ (Fig. 10) suggest a linear relation, which permits approximation of both $\mu_s(\lambda)$ and $g(\lambda)$. A least-squares fit of the Mie theory

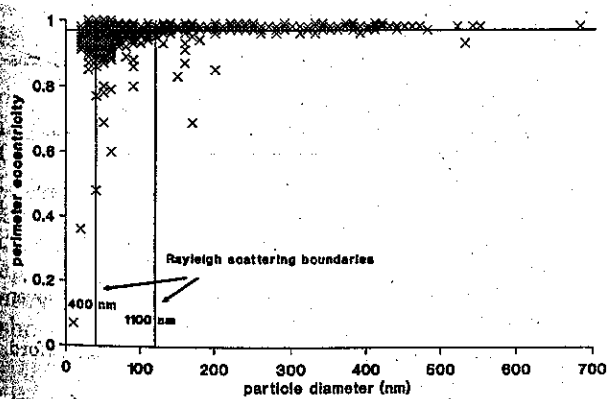

Fig. 8. Plot of data from the form factor calculations for the 1436 measured intralipid particles (sections). The closer the form factor (PE) is to 1, the closer the particles are to a spherical shape (for any nonspherical shape $PE < 1$). The horizontal line ($PE = 0.97$) implies, in case of ellipses, an axis ratio of 0.8 and marks the lower boundary to where the accuracy of the Mie scattering calculations is not significantly influenced.[14] The vertical lines mark the Rayleigh scattering boundaries for the 400-nm ($d = 40$ nm) and 1100-nm ($d = 120$ nm) wavelengths.

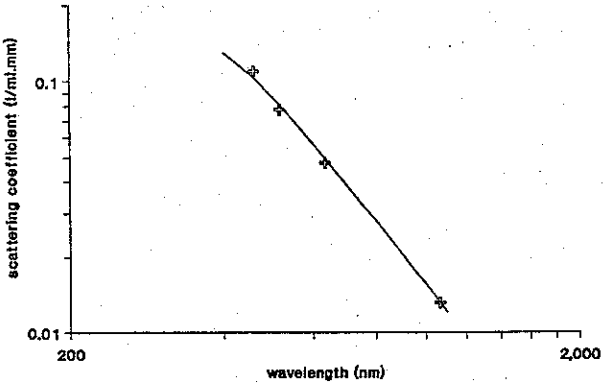

Fig. 9. Calculated scattering coefficient curve (solid line) compared with experimental values (crosses) of Intralipid-10%.

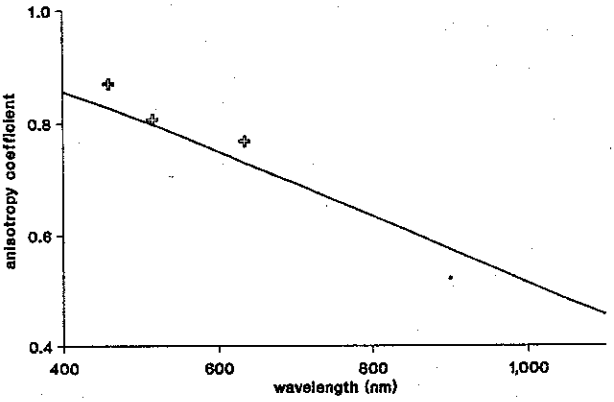

Fig. 10. Calculated anisotropy coefficient (solid line) compared with experimental values (crosses, P3 approximation) of Intralipid-10%.

data yields the equations

$$\mu_s(\lambda) = 0.016\lambda^{-2.4} \quad (\pm 6\%), \tag{12}$$

$$g(\lambda) = 1.1 - 0.58\lambda \quad (\pm 5\%), \tag{13}$$

for $0.4 < \lambda < 1.1$, where λ is in micrometers and μ_s is in units of $\mathrm{mL^{-1}\,L\,mm^{-1}}$. The uncertainties quoted in Eqs. (12) and (13) indicate the maximum deviations from the experimental results (for μ_s at 1064-nm and for g at 632.8-nm wavelengths).

The Mie calculations show that the 150- and 250-nm diameter particles, for, respectively, the 400- and 1100-nm wavelengths, contribute most to μ_s and g. In connection with the particle density [3.97×10^{19} $\mathrm{m^{-3}}$ for Intralipid-10%, Eq. (11)] this implies that the calculated values hold for concentrations up to ~17% Intralipid-10% for the 400-nm wavelength and 4% Intralipid-10% for the 1100-nm wavelength, where these most effective scatterers have a particle spacing of approximately 3–4 particle diameters.

IV. Discussion

From the results of Table I there appears to be good agreement between the experimental data and the Mie theory results for the scattering and the anisot-

ropy coefficients (differences <6%, P3 approximation). Above 514.5 nm the P1 approximation for g and μ_a starts to become less applicable. Differences between our results and the results reported by Moes *et al.*,[1] Star *et al.*,[2] and Flock *et al.*[4] are attributed at least in part to a difference in Intralipid-10% composition. The differences in different preparations of Intralipid-10% may be a disadvantage for choosing it as a tissue phantom.

The mean particle diameter [97(3) nm] found from the particle size distribution determined by electron microscopy (Fig. 7) is a factor of 10 smaller than that found with a Coulter counter measurement by Moes *et al.* [1.0(1) μm].[1] A correction of the electron-microscopy distribution for the splitting of the particles will only slightly displace the distribution to higher sizes [the mean will still be ≈100(10) nm]. This distribution thus proves that the Coulter counter technique is inadequate.

However, a correction for this distribution was omitted for various reasons:

(a) The larger particle sections are already overrepresented in this distribution, because the (numerous) particle sections below ≈20-nm diameter have been disregarded on the electron-microscopy photographs and the particle sections have been classified in only 14 particle sizes. Thus this distribution is at least partly compensated (or even overcompensated) for the absence of a correction.

(b) The chance of particle splitting is believed to be nonhomogeneously distributed along a particle's radius, which makes a correction difficult, if not impossible.

(c) As the particles are not perfect spheres (Fig. 8), this complicates such a correction.

When the distribution would have been corrected for the splitting of the particles, this would have resulted in 10–15% higher values for the calculated scattering and anisotropy coefficients. Also, the data of the particle size histogram could not be reliably fitted to a continuous distribution (negative exponential γ and Deirmendjian distributions were considered).

V. Conclusions

The experimental values for the scattering parameters of Intralipid-10% were found to be within 6% of the Mie theory values and their approximations:

$$\mu_s(\lambda) = 0.016\lambda^{-2.4}, \qquad g(\lambda) = 1.1 - 0.58\lambda$$

for $0.4 < \lambda < 1.1$, where λ is in micrometers and μ_s is in units of mL^{-1} L mm^{-1}. The calculated values will hold for a maximum concentration range from ~17% to ~4% Intralipid-10% for the wavelength range of 400–1100 nm.

The authors thank A. Steenbeek of the Mechanical Department, Academic Medical Center, Amsterdam, for his skillful contribution to the realization of the apparatus; and J. R. Zijp of the State University Groningen (Groningen, The Netherlands), who contributed his computer program for the Mie calculations. These investigations in the program of the Foundation for Fundamental Research on Matter have been supported (in part) by the Netherlands Technology Foundation under grant VNS88.1426.

Address correspondence to M. J. C. van Gemert.

References

1. C. J. M. Moes, M. J. C. van Gemert, W. M. Star, J. P. A. Marijnissen, and S. A. Prahl, "Measurements and calculations of the energy fluence rate in a scattering and absorbing phantom at 633 nm," Appl. Opt. **28,** 2292–2296 (1989).
2. W. M. Star, J. P. A. Marijnissen, H. Jansen, M. Keijzer, and M. J. C. van Gemert, "Light dosimetry for photodynamic therapy by whole bladder wall irradiation," Photochem. Photobiol. **46,** 619–624 (1987).
3. M. J. C. van Gemert, M. C. Berenbaum, and G. H. M. Gijsbers, "Wavelength and light-dose dependence in tumor phototherapy with haematoporphyrin derivative," Br. J. Cancer **52,** 43–49 (1985).
4. S. T. Flock, S. L. Jacques, B. C. Wilson, W. M. Star, and M. J. C. van Gemert, "The optical properties of Intralipid: a phantom medium for light propagation studies," submitted to Lasers Surg. Med.
5. A. Ishimaru, *Wave Propagation and Scattering in Random Media* (Academic, New York, 1978), Vol. 1.
6. W. M. Star, "Comparing the P3-approximation with diffusion theory and with Monte Carlo calculations of light propagation in a slab geometry," in *Dosimetry of Laser Radiation in Medicine and Biology,* G. J. Müller and D. H. Sliney, eds., Soc. Photo-Opt. Instrum. Eng. Inst. Ser. **I55,** 146–154 (1989).
7. W. M. Star and J. P. A. Marijnissen, "Calculating the response of isotropic light dosimetry probes as a function of the tissue refractive index," Appl. Opt. **28,** 2288–2291 (1989).
8. J. H. M. Willison and A. J. Rowe, *Practical Methods in Electron Microscopy* (North-Holland, Amsterdam, 1980), Vol. 8.
9. M. A. Williams, *Quantitative Methods in Biology,* A. M. Glauert, ed., Vol. 6 of Practical Methods in Electron Microscopy (North-Holland, Amsterdam, 1977).
10. R. C. Weast, ed., *Handbook of Chemistry and Physics* (CRC, Boca Raton, Fla., 1978).
11. The Merck Index (Merck, Rahway, N.J., 1976).
12. L. Stryer, *Biochemistry* (Freeman, San Francisco, Calif., 1981).
13. A. L. Aden and M. Kerker, "Scattering of electromagnetic waves from two concentric spheres," J. Appl. Phys. **22,** 1242–1246 (1951).
14. H. C. van de Hulst, *Light Scattering by Small Particles* (Dover, New York, 1981).
15. M. Born and E. Wolf, *Principles of Optics* (Pergamon, Oxford, 1975).
16. G. Yoon, A. J. Welch, M. Motamedi, and M. J. C. van Gemert, "Development and application of three-dimensional light distribution model for laser irradiated tissue," IEEE J. Quantum Electron. **23,** 1721–1733 (1987).